
Faithful Inversion of Generative Models for Effective Amortized Inference

Stefan Webb*
University of Oxford

Adam Goliński
University of Oxford

Robert Zinkov
UBC

N. Siddharth
University of Oxford

Tom Rainforth
University of Oxford

Yee Whye Teh
University of Oxford

Frank Wood
UBC

Abstract

Inference amortization methods share information across multiple posterior-inference problems, allowing each to be carried out more efficiently. Generally, they require the inversion of the dependency structure in the generative model, as the modeller must learn a mapping from observations to distributions approximating the posterior. Previous approaches have involved inverting the dependency structure in a heuristic way that fails to capture these dependencies correctly, thereby limiting the achievable accuracy of the resulting approximations. We introduce an algorithm for faithfully, and minimally, inverting the graphical model structure of any generative model. Such inverses have two crucial properties: a) they do not encode any independence assertions that are absent from the model and b) they are local maxima for the number of true independencies encoded. We prove the correctness of our approach and empirically show that the resulting minimally faithful inverses lead to better inference amortization than existing heuristic approaches.

1 Introduction

Evidence from human cognition suggests that the brain reuses the results of past inferences to speed up subsequent related queries (Gershman & Goodman, 2014). In the context of Bayesian statistics, it is reasonable to expect that, given a generative model, $p(\mathbf{x}, \mathbf{z})$, over data \mathbf{x} and latent variables \mathbf{z} , inference on $p(\mathbf{z} | \mathbf{x}_1)$ is informative about inference on $p(\mathbf{z} | \mathbf{x}_2)$ for two related inputs, \mathbf{x}_1 and \mathbf{x}_2 . Several algorithms (Kingma & Welling, 2014; Rezende et al., 2014; Stuhlmüller et al., 2013; Paige & Wood, 2016; Le et al., 2017, 2018; Maddison et al., 2017a; Naesseth et al., 2018) have been developed with this insight to perform *amortized inference* by learning an inference artefact $q(\mathbf{z} | \mathbf{x})$, which takes as input the values of the observed variables, and—typically with the use of neural network architectures—return a distribution over the latent variables approximating the posterior. These inference artefacts are known variously as inference networks, recognition models, probabilistic encoders, and guide programs; we will adopt the term *inference networks* throughout.

Along with conventional fixed-model settings (Stuhlmüller et al., 2013; Le et al., 2017; Ritchie et al., 2016; Paige & Wood, 2016), a common application of inference amortization is in the training of variational auto-encoders (VAEs) (Kingma & Welling, 2014), for which the inference network is simultaneously learned alongside a generative model. It is well documented that deficiencies in the expressiveness or training of the inference network can also have a knock-on effect on the learned generative model in such contexts (Burda et al., 2016; Cremer et al., 2017, 2018; Rainforth et al., 2018), meaning that poorly chosen coarse-grained structures can be particularly damaging.

Implicit in the factorization of the generative model and inference network in both fixed and learned model settings are probabilistic graphical models, commonly Bayesian networks (BNs), encoding dependency structures. We refer to these as the *coarse-grain* structure, in opposition to the *fine-grain* structure of the neural networks that form each inference (and generative) network factor. In this sense, amortized inference can be framed as the problem of graphical model inversion—how to invert the graphical model of the generative model to give a graphical model approximating the posterior.

*Correspondence to info@stefanwebb.me

Many models from the deep generative modeling literature can be represented as BNs (Krishnan et al., 2017; Gan et al., 2015; Neal, 1990; Kingma & Welling, 2014; Germain et al., 2015; van den Oord et al., 2016b,a), and fall within this framework.

In this paper, we borrow ideas from the probabilistic graphical models literature, to address the previously open problem of how best to automate the design of the coarse-grain structure of the inference network (Ritchie et al., 2016). Typically, the inverse graphical model is formed heuristically. At the simplest level, some methods just invert the edges in the BN for the generative model, removing edges between observed variables (Kingma & Welling, 2014; Gan et al., 2015; Ranganath et al., 2015). In a more principled, but still heuristic, approach, Stuhlmüller et al. (2013); Paige & Wood (2016) construct the inference network by inverting the edges and additionally connecting the parents of children in the original graph (both of which are a subset of a variable’s Markov blanket; see Appendix C).

In general, these heuristic methods introduce conditional independencies into the inference network that are not present in the original distribution. Consequently, they cannot represent the true posterior even in the limit of infinite neural network capacities. Take the simple generative model with branching structure of Figure 1a. The inference network formed by Stuhlmüller’s method inverts the edges of the model as in Figure 1b. However, an inference network that is able to represent the true posterior requires extra edges between the branches, as in Figure 1c.

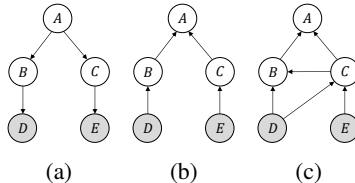


Figure 1: (a) Generative model BN; (b) Inverse BN by Stuhlmüller’s Algorithm; (c) *Faithful* inverse BN by our algorithm.

Another approach, taken by Le et al. (2017), is to use a fully connected BN for the inverse graphical model, such that every

random choice made by the inference network depends on every previous one. Though such a model is expressive enough to correctly represent the data given infinite capacity and training time, it ignores substantial available information from the forward model, inevitably leading to reduced performance for finite training budgets and/or network capacities.

In this paper, we develop a tractable framework to remedy these deficiencies: the *Natural Minimal I-map* generator (NaMI). Given an arbitrary BN structure, NaMI can be used to construct an inverse BN structure that is provably both *faithful* and *minimal*. It is faithful in that it contains sufficient edges to avoid encoding conditional independencies absent from the model. It is minimal in that it does not contain any unnecessary edges; i.e., removing any edge would result in an unfaithful structure.

NaMI chiefly draws upon variable elimination (Koller & Friedman, 2009, Ch 9,10), a well-known algorithm from the graphical model literature for performing exact inference on discrete factor graphs. The key idea in the operation of NaMI is to simulate variable elimination steps as a tool for successively determining a minimal, faithful, and natural inverse structure, which can then be used to parametrize an inference network. NaMI further draws on ideas such as the min-fill heuristic (Fishelson & Geiger, 2004), to choose the ordering in which variable elimination is simulated, which in turn influences the structure of the generated inverse.

To summarize, our key contributions are:

- i) framing generative model learning through amortized variational inference as a graphical model inversion problem, and
- ii) using the simulation of exact inference algorithms to construct an algorithm for generating provably minimally faithful inverses.

Our work thus highlights the importance of constructing both minimal and faithful inverses, while providing the first approach to produce inverses satisfying these properties.

2 Method

Our algorithm builds upon the tools of *probabilistic graphical models*— a summary for unfamiliar readers is given in Appendix A.

2.1 General idea

Amortized inference algorithms make use of inference networks that approximate the posterior. To be able to represent the posterior accurately, the distribution of the inference network should not encode independence assertions that are absent from the generative model. An inference network that did

encode additional independencies could not represent the true posterior, even in the non-parametric limit, with neural network factors whose capacity approaches infinity.

Let us define a *stochastic inverse* for a generative model $p(\mathbf{x}|\mathbf{z})p(\mathbf{z})$ that factors according to a BN structure \mathcal{G} to be a factorization of $q(\mathbf{z}|\mathbf{x})q(\mathbf{x})$ over \mathcal{H} (Stuhlmüller et al., 2013; Paige & Wood, 2016). The $q(\mathbf{z}|\mathbf{x})$ part of the stochastic inverse will define the factorization, or rather, coarse-grain structure, of the inference network. Recall from §1 that this involved two characteristics. We first require \mathcal{H} to be an *I-map* for \mathcal{G} :

Definition 1. Let \mathcal{G} and \mathcal{H} be two BN structures. Denote the set of all conditional independence assertions made by a graph, \mathcal{K} , as $\mathcal{I}(\mathcal{K})$. We say \mathcal{H} is an *I-map* for \mathcal{G} if $\mathcal{I}(\mathcal{H}) \subseteq \mathcal{I}(\mathcal{G})$.

To be an I-map for \mathcal{G} , \mathcal{H} may not encode all the independencies that \mathcal{G} does, but it must not mislead us by encoding independencies not present in \mathcal{G} . We term such inverses as being *faithful*. While the aforementioned heuristic methods *do not* in general produce faithful inverses, using either a fully-connected inverse, or our method, does.

Second, since a fully-connected graph encodes no conditional independencies and is therefore suboptimal, we require in addition that \mathcal{H} be a *minimal I-map* for \mathcal{G} :

Definition 2. A graph \mathcal{K} is a *minimal I-map* for a set of independencies \mathcal{I} if it is an I-map for \mathcal{I} and if removal of even a single edge from \mathcal{K} renders it not an I-map.

We call such inverses *minimally faithful*, which roughly means that the inverse is a local optimum in the number of true independence assertions it encodes.

There will be many minimally faithful inverses for \mathcal{G} , each with a varying number of edges. Our algorithm produces a *natural inverse* in the sense that it either inverts the order of the random choices from that of the generative model (when it is run in the topological mode), or it preserves the ordering of the random choices (when it is run in reverse topological mode):

Definition 3. A stochastic inverse \mathcal{H} for \mathcal{G} over variables \mathcal{X} is a natural inverse if either, for all $X \in \mathcal{X}$ there are no edges in \mathcal{H} from X to its descendants in \mathcal{G} , or, for all $X \in \mathcal{X}$ there are no edges in \mathcal{H} from X to its ancestors in \mathcal{G} .

Essentially, a natural inverse is one for which if we were to perform ancestral sampling, the variables would be sampled in either a topological or reverse-topological ordering, relative to the original model. Consider the inverse networks of \mathcal{G} shown in Figure 2. \mathcal{H}_1 is not a natural inverse of \mathcal{G} , since there is both an edge $A \rightarrow C$ from a parent to a child, and an edge $C \rightarrow B$ from a child to a parent, relative to \mathcal{G} . However, \mathcal{H}_2 and \mathcal{H}_3 are natural, as they correspond respectively to the reverse-topological and topological orderings C, B, A and B, A, C .

Most heuristic methods, including those of (Stuhlmüller et al., 2013; Paige & Wood, 2016), produce (unfaithful) natural inverses that invert the order of the random choices, giving a reverse-topological ordering.

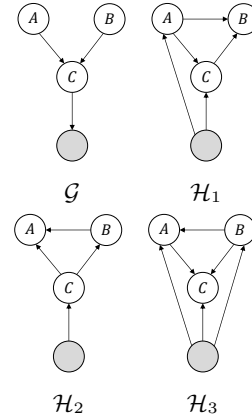


Figure 2: Illustrating definition of naturalness.

2.2 Obtaining a natural minimally faithful inverse

We now present NaMI’s graph inversion procedure that given an arbitrary BN structure, \mathcal{G} , produces a natural minimal I-map, \mathcal{H} . We illustrate the procedure step-by-step on the example given in Figure 3. Here H and J are observed, as indicated by the shaded nodes. Thus, our latent variables are $\mathbf{Z} = \{D, I, G, S, L\}$, our data is $\mathbf{X} = \{H, J\}$, and a factorization for $p(\mathbf{z} | \mathbf{x})$ is desired.

The NaMI graph-inversion algorithm is traced in Table 1. Each step incrementally constructs two graphs: an *induced graph* \mathcal{J} and a *stochastic inverse* \mathcal{H} . The induced graph is an undirected graph whose maximally connected subgraphs, or *cliques*, correspond to the scopes of the intermediate factors produced by simulating variable elimination. The stochastic inverse represents our eventual target which encodes the inverse dependency structure. It is constructed using information from the partially-constructed induced graph. Specifically, NaMI goes through the following steps for this example.

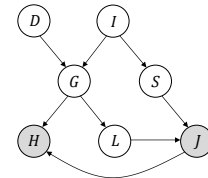


Figure 3: Example BN

STEP 0: The partial induced graph and stochastic inverse are initialized. The initial induced graph is formed by taking the directed graph for the forward model, \mathcal{G} , removing the directionality of the

Table 1: Tracing the NaMI algorithm on example from Figure 3. S is the set of “frontier” variables that are considered for elimination, $v \in S$ the variable eliminated at each step chosen by the greedy min-fill heuristic, \mathcal{J} the partially constructed induced graph *after* each step with black nodes indicating a eliminated variables, and \mathcal{H} the partially constructed stochastic inverse.

STEP	S	v	\mathcal{J}	\mathcal{H}	STEP	S	v	\mathcal{J}	\mathcal{H}
0	\emptyset	\emptyset			3	G, S	S		
1	D, I	D			4	G	G		
2	I	I			5	L	L		

edges, and adding additional edges between variables that share a child in \mathcal{G} —in this example, edges $D - I$, $S - L$ and $G - J$. This process is known as *moralization*. The stochastic inverse begins as disconnected variables, and edges are added to it at each step.

STEP 1: The frontier set of variables to consider for elimination, S , is initialized to the latent variables having no latent parents in \mathcal{G} , that is, D, I . To choose which variable to eliminate first, we apply the greedy min-fill heuristic, which is to choose the (possibly non-unique) variable that adds the fewest edges to the induced graph \mathcal{J} in order to produce as compact an inverse as possible under the topological ordering. Specifically, noting that the cliques of \mathcal{J} correspond to the scopes of intermediate factors during variable elimination, we want to avoid producing intermediate factors which would require us to add additional edges to \mathcal{J} , as doing so will in turn induce additional edges in \mathcal{H} at future steps. For this example, if we were to eliminate D , that would produce an intermediate factor, $\psi_D(D, I, G)$, while if we were to eliminate I , that would produce an intermediate factor, $\psi_I(I, D, G, S)$. Choosing to eliminate would I thus requires adding an edge $G-S$ to the induced graph, as there is no clique I, D, G, S in the current state of \mathcal{J} . Conversely, eliminating D does not require adding extra edges to \mathcal{J} and so we choose to eliminate D .

The elimination of D is simulated by marking its node in \mathcal{J} . The parents of D in the inverse \mathcal{H} are set to be its nonmarked neighbours in \mathcal{J} , that is, I and G . D is then removed from the frontier, and any non-observed children in \mathcal{G} of D whose parents have all been marked added to it—in this case, there are none as the only child of D , G , still has an unmarked parent I .

STEP 2: Variable I is the sole member of the frontier and is chosen for elimination. The elimination of I is simulated by marking its node in \mathcal{J} and adding the additional edge $G-S$. This is required because elimination of I requires the addition of a factor, $\psi_I(I, G, S)$, that is not currently present in \mathcal{J} . The parents of I in the inverse \mathcal{H} are set to be its nonmarked neighbours in \mathcal{J} , G and S . I is then removed from the frontier. Now, G and S are children of I , and both their parents D and I have been marked. Therefore, they are added to the frontier.

STEP 3-5: The process is continued until the end of the fifth step when all the latent variables, D, I, S, G, L , have been eliminated and the frontier is empty. At this point, \mathcal{H} represents a factorization $p(\mathbf{z} | \mathbf{x})$, and we stop here as only a factorization for the posterior is required for amortized inference. Note, however, that it is possible to continue simulating steps of variable elimination on the observed variables to complete the factorization as $p(\mathbf{z} | \mathbf{x})p(\mathbf{x})$.

An important point to note is that NaMI’s graph inversion can be run in one of two modes. The “topological mode,” which we previously implicitly considered, simulates variable elimination in a topological ordering, producing an inverse that reverses the order of the random choices from the generative model. Conversely, NaMI’s graph inversion can also be run in “reverse topological

mode,” which simulates variable elimination in a reverse topological ordering, producing an inverse that preserves the order of random choices in the generative model. We will refer to these approaches as *forward-NaMI* and *reverse-NaMI* respectively in the rest of the paper. The rationale for these two modes is that, though they both produce minimally faithful inverses, one may be substantially more compact than the other, remembering that minimality only ensures a local optimum. For an arbitrary graph, it cannot be said in advance which ordering will produce the more compact inverse. However, as the cost of running the inversion algorithm is low, it is generally feasible to try and pick the one producing a better solution.

Algorithm 1 NaMI Graph Inversion

```

1: Input: BN structure  $\mathcal{G}$ , latent variables  $\mathcal{Z}$ , TOPMODE?
2:  $\mathcal{J} \leftarrow \text{MORALIZE}(\mathcal{G})$ 
3: Set all vertices of  $\mathcal{J}$  to be unmarked
4:  $\mathcal{H} \leftarrow \{\text{VARIABLES}(\mathcal{G}), \emptyset\}$ , i.e. unconnected graph
5: UPSTREAM  $\leftarrow$  “parent” if TOPMODE? else “child”
6: DOWNSTREAM  $\leftarrow$  “child” if TOPMODE? else “parent”
7:  $S \leftarrow$  all latent variables without UPSTREAM latents in  $\mathcal{G}$ 
8: while  $S \neq \emptyset$  do
9:   Select  $v \in S$  according to min-fill criterion
10:  Add edges in  $\mathcal{J}$  between unmarked neighbours of  $v$ 
11:  Make unmarked neighbours of  $v \in \mathcal{J}$ ,  $v$ ’s parents in  $\mathcal{H}$ 
12:  Mark  $v$  and remove from  $S$ 
13:  for unmarked latents DOWNSTREAM  $u$  of  $v$  in  $\mathcal{G}$  do
14:    Add  $u$  to  $S$  if all its UPSTREAM latents in  $\mathcal{G}$  are marked
15:  end for
16: end while
17: return  $\mathcal{H}$ 

```

The general NaMI graph-reversal procedure is given in Algorithm 1. It is further backed up by the following formal demonstration of correctness, the proof for which is given in Appendix F.

Theorem 1. *The Natural Minimal I-Map Generator of Algorithm 1 produces inverse factorizations that are natural and minimally faithful.*

We further note that NaMI’s graph reversal has a running time of order $O(nc)$ where n is the number of latent variables in the graph and $c \ll n$ is the size of the largest clique in the induced graph. We consequently see that it can be run cheaply for practical problems: the computational cost of generating the inverse is generally dominated by that of training the resulting inference network itself. See Appendix F for more details.

2.3 Using the faithful inverse

Once we have obtained the faithful inverse structure \mathcal{H} , the next step is to use it to learn an inference network, $q_\psi(\mathbf{z} \mid \mathbf{x})$. For this, we use the factorization given by \mathcal{H} . Let τ denote the reverse of the order in which variables were selected for elimination by Line 9 in Algorithm 1, such that τ is a permutation of $1, \dots, n$ and $\tau(n)$ is the first variable eliminated. \mathcal{H} encodes the factorization

$$q_\psi(\mathbf{z} \mid \mathbf{x}) = \prod_{i=1}^n q_i(z_{\tau(i)} \mid \text{Pa}_{\mathcal{H}}(z_{\tau(i)})) \tag{1}$$

where $\text{Pa}_{\mathcal{H}}(z_{\tau(i)}) \subseteq \{\mathbf{x}, z_{\tau(1)}, \dots, z_{\tau(i-1)}\}$ indicates the parents of $z_{\tau(i)}$ in \mathcal{H} . For each factor q_i , we must decide both the class of distributions for $z_{\tau(i)} \mid \text{Pa}_{\mathcal{H}}(z_{\tau(i)})$, and how the parameters for that class are calculated. Once learned, we can both sample from, and evaluate the density of, the inference network for a given dataset by considering each factor in turn.

The most natural choice for the class of distributions for each factor is to use the same distribution family as the corresponding variable in the generative model, such that the supports of these distributions match. For instance, continuing the example from Figure 3, if $D \sim N(0, 1)$ in the generative model, then a normal distribution would also be used for $D \mid I, G$ in the inference network. To establish the mapping from data to the parameters to this distribution, we train neural networks using stochastic gradient ascent methods. For instance, we could set $D \mid \{I = i, G = g\} \sim N(\mu_\varphi(i, g), \sigma_\varphi(i, g))$, where μ_φ and σ_φ are two densely connected feedforward networks, with learnable parameters φ . In general, it will be important to choose architectures which well match the problem at hand. For example, when perceptual inputs such as images and language are present in the conditioning variables, it is advantageous to first embed them to a lower-dimensional representation using, for example, convolutional neural networks.

Matching the distribution families in the inference network and generative model, whilst a simple and often adequate approximation, can be suboptimal. For example, suppose that for a normally distributed variable in the generative model, the true conditional distribution in the posterior for that variable is multimodal. In this case, using a (single mode) normal factor in the inference network would not suffice. One could straightforwardly instead use, for example, either a mixture of Gaussians, or, normalizing flows (Rezende & Mohamed, 2015; Kingma et al., 2016), to parametrize each inference network factor in order to improve expressivity, at the cost of additional implementational

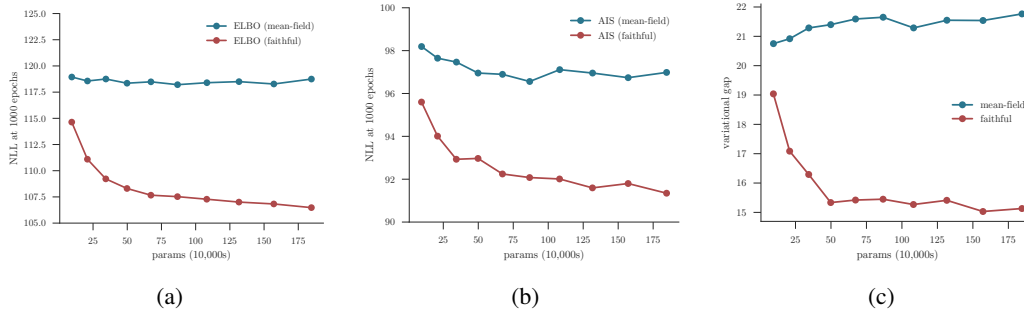


Figure 4: Results for the relaxed Bernoulli VAE with 30 latent units, compared after 1000 epochs of learning the: (a) negative ELBO, and (b) negative AIS estimates, varying inference network factorizations and capacities (total number of parameters); (c) An estimate of the variational gap, that is, the difference between marginal log-likelihood and the ELBO.

complexity. In particular, if one were to use a provably universal density estimator to parameterize each inference network factor, such as that introduced in Huang et al. (2018), the resulting NaMI inverse would constitute a universal density estimator of the true posterior.

After the inference network has been parametrized, it can be trained in number of different ways, depending on the final use case of the network. For example, in the context of amortized stochastic variational inference (SVI) methods such as VAEs (Kingma & Welling, 2014; Rezende et al., 2014), the model $p_\theta(\mathbf{x}, \mathbf{z})$ is learned along with the inference network $q_\psi(\mathbf{z} | \mathbf{x})$ by optimizing a lower bound on the marginal loglikelihood of the data, $\mathcal{L}_{ELBO} = \mathbb{E}_{q_\psi(\mathbf{z} | \mathbf{x})} [\ln p_\theta(\mathbf{x}, \mathbf{z}) - \ln q_\psi(\mathbf{z} | \mathbf{x})]$. Stochastic gradient ascent can then be used to optimize \mathcal{L}_{ELBO} in the same way a standard VAE, simulating from $q_\psi(\mathbf{z} | \mathbf{x})$ by considering each factor in turn and using reparameterization (Kingma & Welling, 2014) when the individual factors permit doing so.

A distinct training approach is provided when the model $p(\mathbf{x}, \mathbf{z})$ is fixed (Papamakarios & Murray, 2015). Here a proposal is learnt for either importance sampling (Le et al., 2017) or sequential Monte Carlo (Paige & Wood, 2016) by using stochastic gradient ascent to minimize the reverse KL-divergence between the inference network $q_\psi(\mathbf{z} | \mathbf{x})$ and the true posterior $p(\mathbf{z} | \mathbf{x})$. Up to a constant, the objective is given by $\mathcal{L}_{IC} = \mathbb{E}_{p(\mathbf{x}, \mathbf{z})} [-\ln q_\psi(\mathbf{z} | \mathbf{x})]$.

Using a minimally faithful inverse structure typically improves the best inference network attainable and the finite time training performance for both these settings, compared with previous naive approaches. In the VAE setting, this can further have a knock-on effect on the quality of the learned model $p_\theta(\mathbf{x}, \mathbf{z})$, both because a better inference network will give lower variance updates of the generative network (Rainforth et al., 2018) and because restrictions in the expressiveness of the inference network lead to similar restrictions in the generative network (Cremer et al., 2017, 2018).

In deep generative models, the BNs may be much larger than the examples shown here. However, typically at the macro-level, where we collapse each vector to a single node, they are quite simple. When we invert this type of collapsed graph, we must do so with the understanding that the distribution over a vector-valued node in the inverse must express dependencies between all its elements in order for the inference network to be faithful.

3 Experiments

We now consider the empirical impact of using NaMI compared with previous approaches. In §3.1, we highlight the importance of using a faithful inverse in the VAE context, demonstrating that doing so results in a tighter variational bound and a higher log-likelihood. In §3.2, we use NaMI in the fixed-model setting. Here our results demonstrate the importance of using both a faithful and minimal inverse on the efficiency of the learned inference network. Low-level details on the experimental setups can be found in Appendix D and an implementation at <https://git.io/fxVQu>.

3.1 Relaxed Bernoulli VAEs

Prior work has shown that more expressive inference networks give an improvement in amortized SVI on sigmoid belief networks and standard VAEs, relative to using the mean-field approximation (Uria et al., 2016; Maaløe et al., 2016; Rezende & Mohamed, 2015; Kingma et al., 2016). Krishnan et al. (2017) report similar results when using more expressive inverses in deep linear-chain state-space models. It is straightforward to see that any minimally faithful inverse for the standard VAE

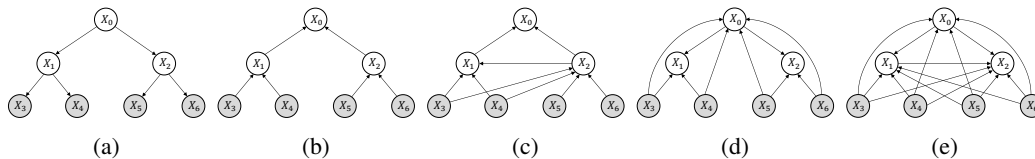


Figure 5: (a) BN structure for a binary tree with $d = 3$; (b) Stuhlmüller’s heuristic inverse; (c) Natural minimally faithful inverse produced by NaMI in topological mode; (d) Most compact inverse when $d > 3$, given by running NaMI in reverse topological mode; (e) Fully connected inverse.

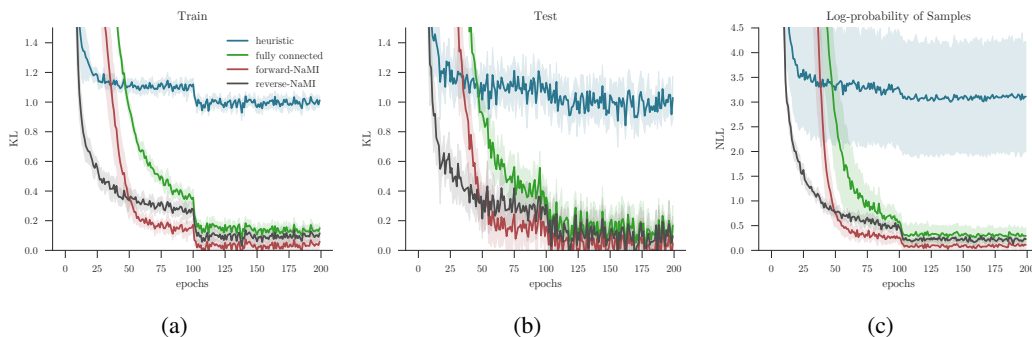


Figure 6: Results for binary tree Gaussian BNs with depth $d = 5$, comparing inference network factorizations in the compiled inference setting. The KL divergence from the analytical posterior estimated to the inference network on the training and test sets are shown in (a) and (b) respectively. (c) shows the average negative log-likelihood of inference network samples under the analytical posterior, conditioning on five held-out data sets. The results are averaged over 10 runs and 0.75 standard deviations indicated. The drop at 100 epochs is due to decimating the learning rate.

framework (Kingma & Welling, 2014) has a fully connected clique over the latent variables so that the inference network can take account of the explaining-away effects between the latent variables in the generative model. As such, both forward-NaMI and backward-NaMI produce the same inverse. The relaxed Bernoulli VAE (Maddison et al., 2017b; Jang et al., 2017) is a VAE variation that replaces both the prior on the latents and the distribution over the latents given the observations with the relaxed Bernoulli distribution (also known as the Concrete distribution). It can also be understood as a “deep” continuous relaxation of sigmoid belief networks.

We learn a relaxed Bernoulli VAE with 30 latent variables on MNIST, comparing a faithful inference network (parametrized with MADE (Germain et al., 2015)) to the mean-field approximation, after 1000 epochs of learning for ten different sizes of inference network, keeping the size of the generative network fixed. We note that the mean-field inference network has the same structure as the heuristic one that reverses the edges from the generative model. A tight bound on the marginal likelihood is estimated with annealed importance sampling (AIS) (Neal, 1998; Wu et al., 2017).

The results shown in Figure 4 indicate that using a faithful inverse on this model produces a significant improvement in learning over the mean-field inverse. Note that the x-axis indicates the number of parameters in the inference network. We observe that for *every* capacity level, the faithful inference network has a lower negative ELBO and AIS estimate than that of the mean-field inference network. In Figure 4c, the variational gap is observed to decrease (or rather, the variational bound tightens) for the faithful inverse as its capacity is increased, whereas it increases for the mean-field inverse. This example illustrates the inadequacy of the mean-field approximation in certain classes of models, in that it can result in significantly underutilizing the capacity of the model.

3.2 Binary-tree Gaussian BNs

Gaussian BNs are a class of models in which the conditional distribution of each variable is normally distributed, with a fixed variance and a mean that is a fixed linear combination of its parents plus an offset. We consider here Gaussian BNs with a binary-tree structured graph and observed leaves (see Figure 5a for the case of depth, $d = 3$). In this class of models, the exact posterior can be calculated analytically (Koller & Friedman, 2009, §7.2) and so it forms a convenient test-bed for performance.

The heuristic inverses simply invert the edges of the graph (Figure 5b), whereas a natural minimally faithful inverse requires extra edges between subtrees (e.g. Figure 5c) to account for the influence one

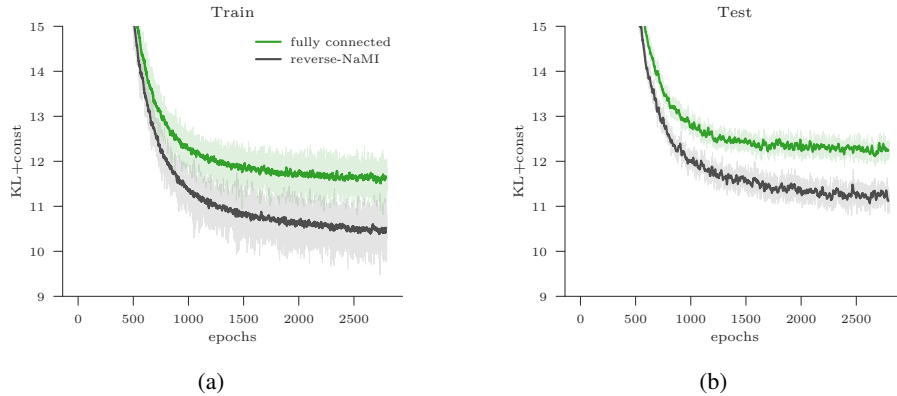


Figure 7: Convergence of reverse KL divergence (used as the training objective) for Bayesian GMM for $K = 3$ clusters and $N = 200$ data points, comparing inference networks with a fixed generative model. The shaded regions indicate 1 standard error in the estimation.

node can have on others through its parent. For this problem, it turns out that running reverse-NaMI (Figure 5d) produces a more compact inverse than forward-NaMI. This, in fact, turns out to be the most compact possible I-map for any $d > 3$. Nonetheless, all three inversion methods have significantly fewer edges than the fully connected inverse (Figure 5e).

The model is fixed and the inference network is learnt from samples from the generative model, minimizing the “reverse” KL-divergence, namely that from the posterior to the inference network $\text{KL}(p_\theta(\mathbf{z}|\mathbf{x})||q_\psi(\mathbf{z}|\mathbf{x}))$, as per (Paige & Wood, 2016). We compared learning across the inverses produced by using Stuhlmüller’s heuristic, forward-NaMI, reverse-NaMI, and taking the fully connected inverse. The fully connected inference network was parametrized using MADE (Germain et al., 2015), and the forward-NaMI one with a novel MADE variant that modifies the masking matrix to exactly capture the tree-structured dependencies (see Appendix E.2). As the same MADE approaches cannot be used for heuristic and reverse-NaMI inference networks, these were instead parametrized with a separate neural network for each variable’s density function. The inference network sizes were kept constant across approaches.

Results are given in Figure 6 for depth $d = 5$ averaging over 10 runs. Figures 6a and 6b show an estimate of $\text{KL}(p_\theta(\mathbf{z}|\mathbf{x})||q_\psi(\mathbf{z}|\mathbf{x}))$ using the train and test sets respectively. From this, we observe that it is necessary to model at least the edges in an I-map for the inference network to be able to recover the posterior, and convergence is faster with fewer edges in the inference network. Despite the more compact reverse-NaMI inverse converging faster than the forward-NaMI one, the latter seems to converge to a better final solution. This may be because the MADE approach could not be used for the reverse-NaMI inverse, but this is a subject for future investigation nonetheless.

Figure 6c shows the average negative log-likelihood of 200 samples from the inference networks evaluated on the analytical posterior, conditioning on five fixed datasets sampled from the generative model not seen during learning. It is thus a measure of how successful inference amortization has been. All three faithful inference networks have significantly lower variance over runs compared to the unfaithful inference network produced by Stuhlmüller’s algorithm.

We also observed during other experimentation that if one were to decrease the capacity of all methods, learning remains stable in the natural minimally faithful inverse at a threshold where it becomes unstable in the fully connected case and in Stuhlmüller’s inverse.

3.3 Gaussian Mixture Models

Gaussian mixture models (GMMs) are a clustering model where the data $\mathbf{x} = \{x_1, x_2, \dots, x_N\}$ is assumed to have been generated from one of K clusters, each of which has a Gaussian distribution with parameters $\{\mu_j, \Sigma_j\}$, $j = 1, 2, \dots, K$. Each datum, x_i is associated with a corresponding index, $z_i \in \{1, \dots, K\}$ that gives the identity of that datum’s cluster. The indices, $\mathbf{z}' = \{z_i\}$ are drawn i.i.d. from a categorical distribution with parameter ϕ . Prior distributions are placed on $\theta = \{\mu_1, \Sigma_1, \dots, \mu_K, \Sigma_K\}$ and ϕ , so that the latent variables are $\mathbf{z} = \{\mathbf{z}', \theta, \phi\}$. The goal of inference is then to determine the posterior $p(\mathbf{z} | \mathbf{x})$, or some statistic of it.

As per the previous experiment, this falls into the fixed-model setting. We factor the fully-connected inverse as, $q(\theta|x)q(\phi|\theta, \mathbf{x})q(\mathbf{z}'|\phi, \theta, \mathbf{x})$. It turns out that applying reverse-NaMI de-

couples the dependence between the indices, z' , and produces a much more compact factorization, $q(\theta|\mathbf{x}, \phi) \prod_i^N q(z_i|x_i, \phi, \theta)q(\phi|\mathbf{x})$, than either the fully-connected or forward-NaMI inverses for this model. The inverse structure produced by Stuhlmüller’s heuristic algorithm is very similar to the reverse-NaMI structure for this problem and is omitted.

We train our amortization artifact over datasets with $N = 200$ samples and $K = 3$ clusters. The inference network terms with distributions over vectors were parametrized by MADE, and we compare the results for the fully-connected and reverse-NaMI inverses. We hold the neural network capacities constant across methods and average over 10 runs, the results for which are shown in Figure 7. We see that learning is faster for the minimally faithful reverse-NaMI method, relative to the fully-connected inverse, and converges to a better solution, in agreement with the other experiments.

3.4 Minimal and Non-minimal Faithful Inverses

To further examine the hypothesis that a non-minimal faithful inverse has slower learning and converges to a worse solution relative to a minimal one, we performed the setup of Experiment 3.2 with depth $d = 4$, comparing the forward-NaMI network to two additional networks that added 12 and 16 connections to forward-NaMI (holding the total capacity fixed).

The additional edges are shown in Figure 8. Note the regular forward-NaMI edges are omitted for visual clarity. Figure 9 shows the average negative log likelihood (NLL) under the true posterior for samples generated by the inference network, based on 5 datasets not seen during training. It appears that the more edges are added beyond minimality, the slower is the initial learning and convergence is to a worse solution.

To further explain why minimality is crucial, we note that adding additional edges beyond minimality means that there will be factors that condition on variables whose probabilistic influence is blocked by the other variables. This effectively adds an input of random noise into these factors, which is why we then see slower learning and convergence to a worse solution.

4 Discussion

We have presented NaMI, a tractable framework that, given the BN structure for a generative model, produces a natural factorization for its inverse that is a minimal I-map for the model. We have argued that this should be used to guide the design of the coarse-grain structure of the inference network in amortized inference. Having empirically analyzed the implications of using NaMI, we find that it learns better inference networks than previous heuristic approaches. We further found that, in the context of VAEs, improved inference networks have a knock-on effect on the generative network, improving the generative networks as well.

Our framework opens new possibilities for learning structured deep generative models that combine traditional Bayesian modeling by probabilistic graphical models with deep neural networks. This allows us to leverage our typically strong knowledge of which variables effect which others, while not overly relying on our weak knowledge of the exact functional form these relationships take.

To see this, note that if we forgo the niceties of making mean-field assumptions, we can impose arbitrary structure on a generative model simply by controlling its parameterization. The only requirement on the generative network to evaluate the ELBO is that we can evaluate the network density at a given input. Recent advances in normalizing flows (Huang et al., 2018; Chen et al., 2018) mean it is possible to construct flexible and general purpose distributions that satisfy this requirement and are amenable to application of dependency constraints from our graphical model. This obviates the need to make assumptions such as conjugacy as done by, for example, Johnson et al. (2016).

NaMI provides a critical component to constructing such a framework, as it allows one to ensure that the inference network respects the structural assumptions imposed on the generative network, without which a tight variational bound cannot be achieved.

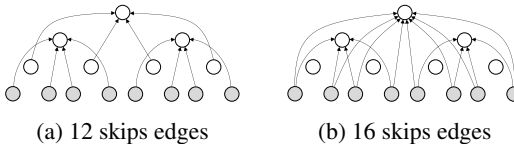


Figure 8: Additional edges over forward-NaMI.

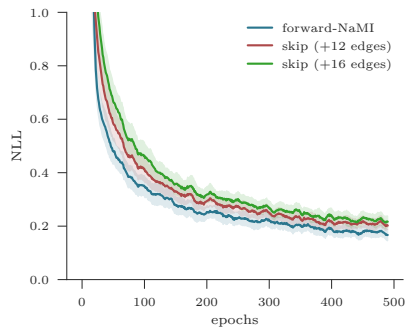


Figure 9: Average NLL of inference network samples under analytical posterior.

Acknowledgments

We would like to thank (in alphabetical order) Rob Cornish, Rahul Krishnan, Brooks Paige, and Hongseok Yang for their thoughtful help and suggestions.

SW and AG gratefully acknowledge support from the EPSRC AIMS CDT through grant EP/L015987/2. RZ acknowledges support under DARPA D3M, under Cooperative Agreement FA8750-17-2-0093. NS was supported by EPSRC/MURI grant EP/N019474/1. TR and YWT are supported in part by the European Research Council under the European Union’s Seventh Framework Programme (FP7/2007–2013) / ERC grant agreement no. 617071. TR further acknowledges support of the ERC StG IDIU. FW was supported by The Alan Turing Institute under the EPSRC grant EP/N510129/1, DARPA PPAML through the U.S. AFRL under Cooperative Agreement FA8750-14-2-0006, an Intel Big Data Center grant, and DARPA D3M, under Cooperative Agreement FA8750-17-2-0093.

References

- Burda, Yuri, Grosse, Roger, and Salakhutdinov, Ruslan. Importance weighted autoencoders. *International Conference on Learning Representations*, 2016.
- Chen, Tian Qi, Rubanova, Yulia, Bettencourt, Jesse, and Duvenaud, David. Neural ordinary differential equations. *arXiv preprint arXiv:1806.07366*, 2018.
- Cremer, Chris, Morris, Quaid, and Duvenaud, David. Reinterpreting importance-weighted autoencoders. *International Conference on Learning Representations Workshop Track*, 2017.
- Cremer, Chris, Li, Xuechen, and Duvenaud, David. Inference suboptimality in variational autoencoders. *Proceedings of the International Conference on Machine Learning*, 2018.
- Fishelson, Maáyan and Geiger, Dan. Optimizing exact genetic linkage computations. *Journal of Computational Biology*, 11(2-3):263–275, 2004.
- Gan, Zhe, Li, Chunyuan, Heno, Ricardo, Carlson, David E, and Carin, Lawrence. Deep temporal sigmoid belief networks for sequence modeling. *Advances in Neural Information Processing Systems*, 2015.
- Germain, Mathieu, Gregor, Karol, Murray, Iain, and Larochelle, Hugo. MADE: masked autoencoder for distribution estimation. *Proceedings of the International Conference on Machine Learning*, 2015.
- Gershman, Samuel J and Goodman, Noah D. Amortized inference in probabilistic reasoning. In *Proceedings of the Annual Conference of the Cognitive Science Society*, 2014.
- Huang, Chin-Wei, Krueger, David, Lacoste, Alexandre, and Courville, Aaron. Neural Autoregressive Flows. *Proceedings of the International Conference on Machine Learning*, 2018.
- Jang, Eric, Gu, Shixiang, and Poole, Ben. Categorical reparameterization with Gumbel-softmax. *International Conference on Learning Representations*, 2017.
- Johnson, Matthew J, Duvenaud, David, Wiltchko, Alexander B, Datta, Sandeep R, and Adams, Ryan P. Composing graphical models with neural networks for structured representations and fast inference. *arXiv preprint arXiv:1603.06277v2 [stat.ML]*, 2016.
- Kingma, Diederik P and Welling, Max. Auto-encoding variational bayes. *International Conference on Learning Representations*, 2014.
- Kingma, Diederik P, Salimans, Tim, and Welling, Max. Improving variational inference with Inverse Autoregressive Flow. *Advances in Neural Information Processing Systems*, 2016.
- Koller, Daphne and Friedman, Nir. *Probabilistic Graphical Models*. MIT Press, 2009. ISBN 9780262013192.
- Krishnan, Rahul G, Shalit, Uri, and Sontag, David. Structured inference networks for nonlinear state space models. *Proceedings of the national conference on Artificial intelligence (AAAI)*, 2017.

- Le, Tuan Anh, Baydin, Atilim Gunes, and Wood, Frank. Inference compilation and universal probabilistic programming. In *Proceedings of the International Conference on Artificial Intelligence and Statistics*, 2017.
- Le, Tuan Anh, Igl, Maximilian, Jin, Tom, Rainforth, Tom, and Wood, Frank. Auto-encoding Sequential Monte Carlo. In *International Conference on Learning Representations*, 2018.
- Maaløe, Lars, Sønderby, Casper Kaae, Sønderby, Søren Kaae, and Winther, Ole. Auxiliary deep generative models. In *Proceedings of the International Conference on Machine Learning*, 2016.
- Maddison, Chris J, Lawson, John, Tucker, George, Heess, Nicolas, Norouzi, Mohammad, Mnih, Andriy, Doucet, Arnaud, and Teh, Yee. Filtering variational objectives. In *Advances in Neural Information Processing Systems*, 2017a.
- Maddison, Chris J, Mnih, Andriy, and Teh, Yee Whye. The Concrete distribution: A continuous relaxation of discrete random variables. In *International Conference on Learning Representations*, 2017b.
- Naesseth, Christian A, Linderman, Scott W, Ranganath, Rajesh, and Blei, David M. Variational Sequential Monte Carlo. In *Proceedings of the International Conference on Artificial Intelligence and Statistics*, 2018.
- Neal, Radford M. Learning stochastic feedforward networks. *Department of Computer Science, University of Toronto*, 1990.
- Neal, Radford M. Annealed Importance Sampling (technical report 9805 (revised)). *Department of Statistics, University of Toronto*, 1998.
- Paige, Brooks and Wood, Frank. Inference networks for Sequential Monte Carlo in graphical models. In *Proceedings of the International Conference on Machine Learning*, 2016.
- Papamakarios, George and Murray, Iain. Distilling intractable generative models. In *Probabilistic Integration Workshop at Neural Information Processing Systems*, 2015.
- Rainforth, Tom, Kosiorek, Adam R, Le, Tuan Anh, Maddison, Chris J, Igl, Maximilian, Wood, Frank, and Teh, Yee Whye. Tighter variational bounds are not necessarily better. *Proceedings of the International Conference on Machine Learning*, 2018.
- Ranganath, Rajesh, Tang, Linpeng, Charlin, Laurent, and Blei, David M. Deep exponential families. In *Proceedings of the International Conference on Artificial Intelligence and Statistics*, 2015.
- Rezende, Danilo and Mohamed, Shakir. Variational inference with normalizing flows. In *Proceedings of the International Conference on Machine Learning*, 2015.
- Rezende, Danilo Jimenez, Mohamed, Shakir, and Wierstra, Daan. Stochastic backpropagation and approximate inference in deep generative models. In *Proceedings of the International Conference on Machine Learning*, 2014.
- Ritchie, Daniel, Horsfall, Paul, and Goodman, Noah D. Deep amortized inference for probabilistic programs. *arXiv preprint arXiv:1610.05735*, 2016.
- Stuhlmüller, Andreas, Taylor, Jacob, and Goodman, Noah. Learning stochastic inverses. In *Advances in Neural Information Processing Systems*, 2013.
- Uria, Benigno, Côté, Marc-Alexandre, Gregor, Karol, Murray, Iain, and Larochelle, Hugo. Neural autoregressive distribution estimation. *Journal of Machine Learning Research*, 17(205):1–37, 2016.
- van den Oord, Aaron, Kalchbrenner, Nal, Espeholt, Lasse, Vinyals, Oriol, Graves, Alex, et al. Conditional image generation with PixelCNN decoders. In *Advances in Neural Information Processing Systems*, 2016a.
- van den Oord, Aaron, Kalchbrenner, Nal, and Kavukcuoglu, Koray. Pixel recurrent neural networks. In *Proceedings of the International Conference on Machine Learning*, 2016b.
- Wu, Yuhuai, Burda, Yuri, Salakhutdinov, Ruslan, and Grosse, Roger. On the quantitative analysis of decoder-based generative models. In *International Conference on Learning Representations*, 2017.

Faithful Inversion of Generative Models for Effective Amortized Inference: Supplementary Material

Stefan Webb*
University of Oxford

Adam Goliński
University of Oxford

Robert Zinkov
UBC

N. Siddharth
University of Oxford

Tom Rainforth
University of Oxford

Yee Whye Teh
University of Oxford

Frank Wood
UBC

A Probabilistic Graphical Models

This summary is based on Koller & Friedman (2009).

A.1 Bayesian networks and representation

Any probability distribution implicitly represents certain independence relationships between its variables via its factorization. These are of interest because they can be exploited to both compactly represent distributions and to reduce the cost of inference. The set of such relationships is defined as:

Definition 1. Let p be a distribution defined over \mathcal{X} . We define $\mathcal{I}(p)$ to be the set of independence assertions of the form $(\mathbf{X} \perp \mathbf{Y} \mid \mathbf{Z})$ that hold in p , where $\mathbf{X}, \mathbf{Y}, \mathbf{Z} \subseteq \mathcal{X}$.

The framework of probabilistic graphical models is used for representing and reasoning about a wide class of probability distributions by making these independence assertions explicit. Distributions are represented as the product of factors over subsets of the model variables. Associated with the factorization is a graph, wherein the nodes are the random variables of the model, and the edges express the distribution’s independence assertions.

Bayesian networks (BNs) are a class of probabilistic graphical models that use a directed acyclic graph. We refer to the graph alone as the BN structure, whereas the BN itself comprises, in addition, a representation for each factor. In a BN, each variable has a conditional distribution that only depends on its parents in the graph. For example, in Figure 2a the distribution factors as $p(a)p(b|a)p(c|a)p(d|b)p(e|c)$.

Formally, the semantics of the BN structure are that it encodes the local independencies:

Definition 2. A Bayesian network structure \mathcal{G} encodes the local independencies $\mathcal{I}_l(\mathcal{G})$, namely, those of the form $X_i \perp \text{NonDescendants}_{X_i} \mid \text{Pa}_{X_i}^{\mathcal{G}}$ for each $X_i \in \mathcal{G}$, where $\text{Pa}_{X_i}^{\mathcal{G}}$ denotes the parents of X_i in \mathcal{G} .

It turns out that there are additional independencies that can be read off \mathcal{G} aside from the local ones, that hold for every p that factorizes over \mathcal{G} , and these are identified by the concept of d -separation.

We relate the conditional independencies encoded in a graph, such as a BN structure, to a corresponding distribution by the concept of an independency map, or I -map:

Definition 3. Let \mathcal{K} be any graph object associated with a set of independencies $\mathcal{I}(\mathcal{K})$. We say that \mathcal{K} is an I -map for a distribution p if $\mathcal{I}(\mathcal{K}) \subseteq \mathcal{I}(p)$.

In our case, a BN structure \mathcal{G} is an I -map for p if $\mathcal{I}_l(\mathcal{G}) \subseteq \mathcal{I}(p)$. This means that \mathcal{G} may not encode all the independencies in p , but it does not mislead us by encoding independencies not present in p . For this reason, we will interchangeably use the expression, “ \mathcal{G} is faithful to p .”

*Correspondence to info@stefanwebb.me

It can be proven that a BN structure \mathcal{G} is an I-map for a distribution p if and only if p is representable as a set of conditional probability distributions (also referred to as model factors), factoring according to \mathcal{G} , that is,

$$P(\mathcal{X}) = \prod_{X_i \in \mathcal{X}} P(X_i \mid \text{Pa}_{X_i}^{\mathcal{G}}).$$

Therefore, we can use the graph as a means of revealing the structure in a distribution.

A.2 D-separation

We give a heuristic explanation of d-separation by examining the opposite question of, roughly speaking, when can probabilistic influence flow from one variable to another.

In paths in \mathcal{G} with three variables that form,

- a causal trail, $X \rightarrow Z \rightarrow Y$,
- an evidential trail, $X \leftarrow Z \leftarrow Y$, or,
- a common cause, $X \leftarrow Z \rightarrow Y$,

knowledge of X is informative about Y when Z is not observed, and observing Z blocks this flow of information. For example, suppose X is the coherence of a course, Z its difficulty, and Y the grade a student receives. Further, suppose there is a causal trail $X \rightarrow Z \rightarrow Y$ in the graph and no other trail between X and Y . If we observe that the course is taught coherently, this will inform our beliefs about its difficulty, which will in turn change our beliefs about the student’s grade. On the other hand, if we observe that it is a difficult course, the coherency of the course will not effect our beliefs about the student’s grade as it can only do so indirectly via the difficulty variable.

Conversely, for a common effect motif, $X \rightarrow Z \leftarrow Y$, also known as a *v-structure*, there is an “explaining away” effect, whereby if we observe Z (or a descendent of Z), then knowledge of X is informative about Y . For example, if X is the difficulty of an exam, Z is a student’s result, and Y is his aptitude, then if we observe a poor result and that the exam is hard, we can attribute the result to the difficulty of the exam, and lessen our belief that the student is incapable.

This heuristic reasoning generalizes to longer trails in the concept of an *active trail*,

Definition 4. Let \mathcal{G} be a BN structure and $X_1 \rightleftharpoons \dots \rightleftharpoons X_n$ a trail in \mathcal{G} . Let \mathbf{Z} be a subset of observed variables. The trail $X_1 \rightleftharpoons \dots \rightleftharpoons X_n$ is active given \mathbf{Z} if,

- Whenever we have a *v-structure* $X_{i-1} \rightarrow X_i \leftarrow X_{i+1}$, then X_i or one of its descendants are in \mathbf{Z} ;
- No other node along the trail is in \mathbf{Z} .

Those subsets of variables, conditioned on another set, are said to be d-separated if an active trail does not exist between them. Formally:

Definition 5. Let $\mathbf{X}, \mathbf{Y}, \mathbf{Z}$ be three sets of nodes in \mathcal{G} .

We say that \mathbf{X} and \mathbf{Y} are d-separated given \mathbf{Z} , denoted $\text{d-sep}_{\mathcal{G}}(\mathbf{X}; \mathbf{Y} \mid \mathbf{Z})$, if there is no active trail between any node $X \in \mathbf{X}$ and $Y \in \mathbf{Y}$ given \mathbf{Z} . We use $\mathcal{I}(\mathcal{G})$ to denote the set of independencies that correspond to d-separation,

$$\mathcal{I}(\mathcal{G}) = \{(\mathbf{X} \perp \mathbf{Y} \mid \mathbf{Z}) \mid \text{d-sep}_{\mathcal{G}}(\mathbf{X}; \mathbf{Y} \mid \mathbf{Z})\}.$$

D-separation is sound in the sense that if \mathbf{X} and \mathbf{Y} are d-separated given \mathbf{Z} in a graph \mathcal{G} , then $\mathbf{X} \perp \mathbf{Y} \mid \mathbf{Z}$ holds in all distributions p that factorize according to \mathcal{G} (Koller & Friedman, 2009, Theorem 3.3).

A certain converse statement also holds for the completeness of d-separation. If \mathbf{X} and \mathbf{Y} are not d-separated given \mathbf{Z} in a graph \mathcal{G} , then $\mathbf{X} \perp \mathbf{Y} \mid \mathbf{Z}$ does not hold for almost all (in a measure theoretic sense) distributions p that factorize according to \mathcal{G} (Koller & Friedman, 2009, Theorem 3.5). So, for all practical purposes one may assume $\mathcal{I}(\mathcal{G}) = \mathcal{I}(p)$.

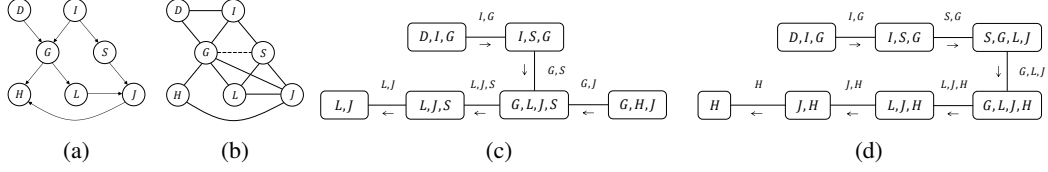


Figure 1: (a) BN structure for “Extended Student” example; (b) the induced graph corresponding to elimination ordering D, I, H, G, S, L ; (c) the corresponding clique tree; (d) the clique tree corresponding to elimination ordering D, I, S, G, L, J, H .

A.3 Exact inference by variable elimination

Variable elimination is an algorithm for performing exact inference in graphical models which have the property that summation of variables in the model factors is tractable—typically ones with discrete finite-valued factors. From a higher perspective, it works by using the observation that we can exchange the order of the summation of the model variables and the multiplication of the model factors based on their scope, i.e. what variables they take as inputs. Doing so can greatly reduce the complexity of summation, or rather inference, if the variable ordering is carefully chosen.

Consider the BN structure from Figure 1a and suppose the task is to compute $P(J)$. Simply multiplying all the factors together, then summing out $\mathcal{X} \setminus \{J\}$,

$$P(J) = \sum_{\mathcal{X} \setminus \{J\}} \prod_{X \in \mathcal{X}} \phi_X,$$

would not be an efficient means to do so. Rather, we ought to exploit the structure in the model, and perform summation on factors with smaller scope. Suppose also, that we perform the summation, or variable elimination, in the ordering D, I, H, G, S, L . To sum out D , we can pull out all factors that do not contain D in their scope. First we multiply the factors depending on D together,

$$\psi_1(D) = \phi_D(D) \phi_G(G, I, D),$$

then sum out D ,

$$\tau_1(G, I) = \sum_D \psi_1,$$

to produce a new intermediate factor that is used in subsequent computations.

Similarly, to sum out I ,

$$\begin{aligned} \psi_2(G, I, S) &= \tau_1(G, I) \phi_I(I) \phi_S(S, I), \\ \tau_2(G, I) &= \sum_I \psi_2. \end{aligned}$$

continuing this process to eliminate the remaining variables. As each intermediate factor, ψ_i , has a scope much narrower than the full variables set, \mathcal{X} , exact inference is made tractable.

A.4 Induced graphs

The computational cost of an application of variable elimination, which depends on the size of the scope of the largest intermediate factor, can be captured in an undirected graph known as the *induced graph*. It is defined as follows:

Definition 6. Let Φ be a set of factors over $\mathcal{X} = \{X_1, \dots, X_n\}$, and \prec be an elimination ordering for some subset $\mathcal{X} \subseteq \mathcal{X}$. The induced graph $\mathcal{I}_{\Phi, \prec}$ is an undirected graph over \mathcal{X} , where X_i and X_j are connected by an edge if they both appear in some intermediate factor ϕ generated by the variable elimination algorithm using \prec as an elimination ordering.

The induced graph for our previous example is given in Figure 1b. We see that it has cliques, or maximally connected subgraphs, for the subsets $\{D, I, G\}$, $\{I, S, G\}$, $\{G, J, S, L\}$, and $\{G, H, J\}$, which correspond to the scopes of some intermediate factor, ψ_i , in the computation.

We can form the induced graph for a given run of variable elimination on \mathcal{G} as follows. First, we “moralize” \mathcal{G} by connecting all its parents and removing the directionality of the edges. This induces an edge between X_i and X_j if they appear in the scope of a model factor $\phi \in \Phi$ before variable elimination. During variable elimination, after we have calculated the scope of each intermediate factor, we add additional edges to the graph, indicated in our figures with dotted edges, so that the scope of each intermediate factor, ψ_i , is maximally connected. For instance, in our example, when eliminating I , a factor $\psi_3(G, I, S)$ occurs, so we must add the additional edge $G - S$. A good variable elimination ordering will add as few additional edges so that the scope of the intermediate factors is constrained.

A.5 Clique trees

Another way to understand the variable elimination algorithm is as an algorithm that passes messages over a tree structure known as a clique tree. Continuing our running “Student” example, the clique tree corresponding to the variable elimination ordering D, I, H, G, S, L is given in Figure 1c. We refer to the nodes in the tree as the cliques, which are subsets of the model variables corresponding to the scopes of the intermediate factors, $\{\psi_i\}$. Each model factor, ϕ_i , is associated to a node in the graph, for example, $\phi_D(D)$, $\phi_G(D, I, G)$, and $\phi_I(I)$ are associated with the node “ D, I, G ,” and $\phi_S(I, S)$ is associated with “ I, S, G .”

The messages, $\{\tau_i\}$, are formed by multiplying together all the factors associated with a node and its incoming messages, and summing out the variables not in the intersection of the node and its downstream neighbour. The intersections of the node scopes are indicated above each edge and are known as the sepsets. The tree is undirected, although we have indicated the directionality of message passing with arrows above each edge.

Formally, a clique tree is defined as follows:

Definition 7. A clique tree \mathcal{U} for a set of factors Φ over \mathcal{X} is an undirected graph, each of whose nodes i is associated with a subset $\mathbf{C}_i \subset \mathcal{X}$. A clique tree must be family-preserving—each factor $\phi \in \Phi$ must be associated with a clique \mathbf{C}_i such that $\text{scope}[\phi] \subseteq \mathbf{C}_i$. Each edge between a pair of cliques \mathbf{C}_i and \mathbf{C}_j is associated with a sepset $\mathbf{S}_{i,j} \subseteq \mathbf{C}_i \cap \mathbf{C}_j$. Also, it must hold that whenever there is a variable X such that $X \in \mathbf{C}_i$ and $X \in \mathbf{C}_j$, then X is also in every clique in the (unique) path in \mathcal{T} between \mathbf{C}_i and \mathbf{C}_j .

An important property of clique trees, known as the *sepset property*, is the following: all variables upstream of a clique are conditionally independent of those downstream, conditioned on the corresponding sepset, and the sepset is the minimal set for which this holds (Koller & Friedman, 2009, Theorem 10.2). In this way, the sepset “separates” upstream and downstream variables. Property 1 in B.4 is equivalent to the sepset property—our definition of “upstream/downstream” coincides in induced graphs and clique trees, and the sepsets are seen to correspond to the downstream neighbours of a variable. Compare the induced graph of §2.2 with its corresponding clique tree in Figure 1d.

A.6 Exact inverses

Is it possible in general for a stochastic inverse \mathcal{H} to perfectly capture the independencies in \mathcal{G} so that $\mathcal{I}(\mathcal{H}) = \mathcal{I}(\mathcal{G})$? The answer is given in the negative by the following theorem and associated definitions (Koller & Friedman, 2009, Theorem 3.8):

Definition 8. The skeleton of a BN structure \mathcal{G} over \mathcal{X} is an undirected graph over \mathcal{X} that contains an edge $\{X, Y\}$ for every edge (X, Y) in \mathcal{G} .

Definition 9. A v -structure $X \rightarrow Y \leftarrow Z$ is an immorality if there is no direct edge between X and Y .

Theorem 1. Let \mathcal{G} and \mathcal{H} be two graphs over \mathcal{X} . Then \mathcal{G} and \mathcal{H} have the same skeleton and the same set of immoralities if and only if $\mathcal{I}(\mathcal{H}) = \mathcal{I}(\mathcal{G})$.

In general, immoralities in \mathcal{G} are destroyed in \mathcal{H} , as both heuristic and faithful inversion methods may reverse edges in v -structures or add a direct edge between their parents.

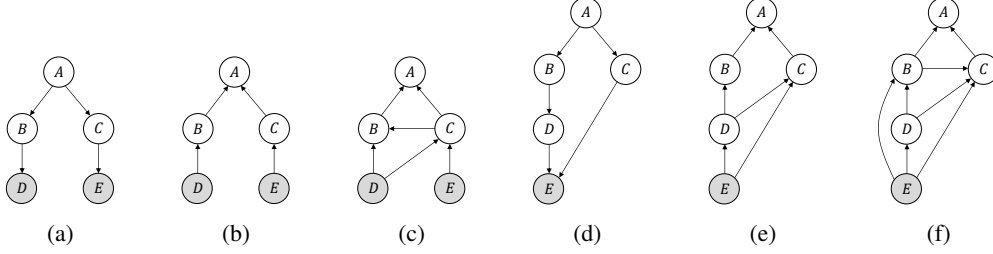


Figure 2: (a,d) Two simple BN structures for a generative model, (b,e) The corresponding inverse BN structures formed by Stuhlmüller’s Algorithm, (c,f) The inverse BN structure formed by our algorithm. This demonstrates how Stuhlmüller’s Algorithm can miss many edges and longer-term dependencies.

B Restrictions on orderings

So far, we have been simulating variable elimination on the latent variables in the model, stopping at the observed ones. In special cases, we may wish to further restrict the variable elimination ordering within the non-observed variables. For instance, the semi-supervised variational objective of Kingma et al. (2014) requires a factorization $q(\mathbf{z}, \mathbf{y} | \mathbf{x}) = q(\mathbf{z} | \mathbf{x}, \mathbf{y})q(\mathbf{y} | \mathbf{x})$, where \mathbf{y} are the semi-observed variables. In this case we should eliminate all \mathbf{z} before eliminating \mathbf{y} . Algorithm 1 can be suitably modified to accommodate this by running Lines 6–17, replacing “latents” and “latent variables” with $z \in \mathbf{z}$, and repeating Lines 6–16 replacing those terms with $y \in \mathbf{y}$. In a time series model, we may wish to eliminate the latent variables in their time ordering, $\mathbf{z}_1, \dots, \mathbf{z}_T$, and can repeat Lines 6–16 T times, replacing those terms with $z \in \mathbf{z}_i$ in turn.

C Counterexamples to Stuhlmüller’s heuristic inversion

Stuhlmüller et al. (2013) give an algorithm for forming a “heuristic inverse,” \mathcal{H} , of a BN structure, \mathcal{G} .

First, let us define the concept of a Markov Blanket in a BN:

Definition 10. *Let \mathcal{G} be a BN structure over \mathcal{X} . Then, the Markov blanket of $X \in \mathcal{X}$ in \mathcal{G} , $\text{Markov}_{\mathcal{G}}(X)$, is the minimal set of variables, \mathbf{Z} , that when conditioned on, make X independent of $\mathcal{X} \setminus X$ —that is, the set of parents, child, and parents of children of X .*

It is necessary to condition on the parents of a variable’s children, because conditioning on its children may activate v-structures, and so we need to condition on the children’s parents to block these paths.

Stuhlmüller’s algorithm works by visiting the variables of \mathcal{G} in a reverse topological ordering, Y_1, \dots, Y_n (where Y_i is equal to some observed X_j or latent Z_k depending on the structure of the graph and the ordering). The graph \mathcal{H} is produced by setting the parents of Y_i to be the intersection of Y_1, \dots, Y_{i-1} and that node’s Markov blanket in \mathcal{G} , excluding latent parents for observed nodes. The procedure is equivalent to reversing the edges in \mathcal{G} , adding extra edges to fully connect all the parents of a node in \mathcal{G} , and removing edges from latent nodes into observed ones. This produces the desired factorization $q(\mathbf{x} | \mathbf{z})q(\mathbf{z})$.

Paige & Wood (2016) claim that a heuristic inverse structure \mathcal{H} is an I-map for \mathcal{G} , or equivalently, by the almost-everywhere completeness of d-separation, that $Y_1 \rightleftharpoons \dots \rightleftharpoons Y_m$ is active in \mathcal{H} given \mathbf{Z} implies that $Y_m \rightleftharpoons \dots \rightleftharpoons Y_1$ is active in \mathcal{G} given \mathbf{Z} , for an arbitrary trail.

If this were true, then we could factor p as,

$$\begin{aligned}
 p(\mathbf{y}) &= \prod_{i=1}^n p(y_i | y_1, \dots, y_{i-1}) \\
 &= \prod_{i=1}^n p(y_i | \{y_1, \dots, y_{i-1}\} \cap \text{Markov}_{\mathcal{G}}(y_i) \cap \mathbb{I}(y_i)),
 \end{aligned}$$

where, $\mathbb{I}(y_i) = \mathbf{z}$ if $y_i \in \mathbf{z}$ and \mathbf{y} otherwise, is defined to prevent edges from latent nodes into observed ones.

The problem is in going from the first to the second line. For example, consider the factor for an arbitrary latent node, Z_i . We have not conditioned on its *complete* Markov blanket—only the children, and parents of children that occur previously in the ordering—and so we cannot assert that Z_i is independent from all the other previous variables.

It is easy to construct counterexamples, for which the influence of a variable flows through one of its parents to effect another variable prior in the ordering that has not been conditioned on. For instance, see Figure 2.

Consider our first example in parts (a-b). The heuristic inverse, \mathcal{H} , in (b) asserts that $B \perp C$, since any path between the two variables is blocked by the v-structure. However, $B \perp C$ does not hold in the model, \mathcal{G} , in (a), as the path $B \leftarrow A \rightarrow C$ is active. As \mathcal{H} asserts a conditional independence relationship that does not hold in \mathcal{G} , it is not faithful to the model. A similar argument can be produced for the second example in parts (d-e). A correct inverse structure produced by our algorithm is given in parts (c) and (f).

D Details of experimental setup

Optimization was performed with Adam (Kingma & Ba, 2014) and the default hyperparameters, $\beta_1 = 0.9$ and $\beta_2 = 0.999$.

D.1 Relaxed Bernoulli VAEs

We perform amortized SVI on a relaxed SBN with 30 latent units on the MNIST data set that has been statically binarized, and use the standard 50,000/10,000/10,000 split for train/test/validation. The relaxed Bernoulli prior had parameter $p = 0.5$ and temperature $\tau = 1/2$, and the relaxed Bernoulli distribution in the inference program, temperature $\tau = 2/3$

A learning rate of $1e-4$ was used, with batch size 100.

In the forward model, $p(\mathbf{x} \mid \mathbf{z})$, the parameters were calculated by a tanh feedforward network with two hidden layers of size [200, 200]. For the ten mean-field inference programs, the same form of feedforward network was used, varying the size of the hidden layers from [100, 100], [200, 200], ..., [1000, 1000]. The ten minimally faithful/fully connected inverses were parametrized similarly, adjusting upwards the size of the different hidden layers to match the number of parameters to the corresponding mean-field program.

The annealed importance sampling (AIS) estimate of $\ln(p(\mathbf{x}))$ averaged 5 chains of 5000 intermediate distributions. As in Maddison et al. (2017, C.3), the latents are treated in the logistic space rather than the relaxed Bernoulli space for numerical stability. We found this was also essential for applying annealed importance sampling.

D.2 Binary tree Gaussian BNs

We model binary tree Gaussian BNs of depth d with distribution, $X_0 \sim N(0, 1)$, $X_i \mid x_{\lfloor(i-1)/2\rfloor} = y \sim N(w_i y, 1)$, $i = 1, \dots, 2^d - 2$, where the $\{w_i\}$ are fixed constants sampled from $U[1/2, 2]$ and we treat the leaves $\{x_{2^{d-1}-1}, \dots, x_{2^d-2}\}$ as the observed variables.

In both the heuristic/Stuhlmüller’s method and most compact inference programs, each inverse factor was parametrized with a normal distribution using a two hidden-layer ReLU feedforward network with [100, 100] and [97, 97] hidden units, respectively, to map from its parents to the distribution parameters.

A ReLU feedforward network with two hidden layers was also used for the fully connected and natural minimally faithful inference programs, with [501, 501] and [1210, 1210] hidden units, respectively. The MADE masks reduce the effective number of parameters, explaining why these numbers are greater than that for the heuristic inference program.

The total number of parameters for the heuristic, fully connected, most compact, and natural inference programs were 160545, 159136, 156021, and 159901, respectively.

The learning rate was initialized to $1e-3$, decimating when learning converged, for example, every 100 epochs in the case of $d = 5$. A batchsize of 250 was used, new samples from the generative

model being drawn every minibatch for training, with 10 minibatches considered to constitute an epoch, and the test objective evaluated on a single minibatch every epoch.

The exact posterior under the true factorization can be calculated by using the equivalence between Gaussian BNs and multivariate normal distributions (Koller & Friedman, 2009, §7.2)—first the forward model is converted to the parameters of a multivariate normal distribution using Theorem 7.3, which is then transformed back into a Gaussian BN for the posterior using our true factorization and Theorem 7.4. Samples from the posterior can be drawn by ancestral sampling.

We evaluate inference amortization by calculating the average log-posterior of a minibatch from the encoders every epoch under five fixed datasets of the observed variables (which have not been seen by the optimizer).

D.3 Bayesian Gaussian Mixture Models

We model a Bayesian Gaussian mixture model with $K = 3$ clusters and $N = 200$ two-dimensional samples. The variance parameters of the clusters were parametrized with $\sigma_{1k}, \sigma_{2k}, \rho_k$, where ρ_k is the correlation between the two dimensions. The inference network terms with distributions over vectors were parametrized by MADE, and each inverse factor was parametrized with a suitable probability distribution— ϕ with a Dirichlet, ρ_k with Kumaraswamy, μ with a mixture of Gaussians, σ_{1k} and σ_{2k} with Inverse Gamma distributions, and z with a Categorical.

The MADEs constituted of two hidden-layer ReLU feedforward network with 360 hidden units per layer for the NaMI inverse and 50 for the fully connected inverse, so that the total number of parameters in the network would be held fixed to allow for a fair comparison. The total number of parameters for the fully connected and natural inference programs were 820047, and 826779, respectively.

The learning rate was initialized to $1e-3$ and Adam algorithm was used. A dataset of 2000 samples was sampled from the generative model for training the inference network, in minibatches of 200. When the validation error decreased, a new dataset was drawn and training continued.

D.4 Minimal and Non-minimal Faithful Inverses

The setup for this experiment was as per D.2 unless stated otherwise. We used a model of depth $d = 4$ rather than $d = 5$, parametrizing the forward-NaMI inverse with separate networks for each conditional distribution, rather than a single tree-MADE network. This was because adding extra edges to forward-NaMI broke the ability to share weights, and we wanted the same parametrization scheme for all three inverses. Each network had two hidden layers of size 100. The two inverses with additional edges over the forward-NaMI one used networks with two hidden layers of size 99 in order to keep the total capacity roughly fixed.

E Neural density estimators for weight-sharing

E.1 MADE

We use the masked autoencoder distribution estimator (MADE) model (Germain et al., 2015) extended for conditional distributions (Paige & Wood, 2016) to model fully connected distributions over latent variables, conditioning on all observations, that is,

$$q(\mathbf{z} \mid \mathbf{x}) = \prod_{i=0}^{m-1} q_i(z_i \mid z_1, \dots, z_{i-1}, \mathbf{x}).$$

From a high level, MADE works by using a single feedforward network that takes as inputs (\mathbf{x}, \mathbf{z}) , and outputs parameters of all the factors $\{q_i\}$. The weights of the feedforward network are multiplied elementwise by masking matrices so that if one were to trace a path back from an output parameter for q_i to the inputs, that parameter would only be connected to $\{z_1, \dots, z_{i-1}, \mathbf{x}\}$.

To make things more concrete, consider a single-hidden-layer feedforward network, used to calculate the parameters, θ , of binary valued data,

$$\begin{aligned}\mathbf{h} &= \sigma_w \left(\mathbf{b} + (W \odot M^{(w)})(\mathbf{z}, \mathbf{x}) \right) \\ \theta &= \sigma_v \left(\mathbf{c} + (V \odot M^{(v)})\mathbf{h} \right),\end{aligned}$$

where $\mathbf{b}, \mathbf{c}, W, V$ are real-valued parameters to be learned, \odot denotes elementwise multiplication, σ_w, σ_v are nonlinear functions, and M_w, M_v are fixed binary masks.

To each hidden unit, h_i , we assign an integer uniformly from $\{1, \dots, m-1\}$. To each input unit we assign the integer 0 if it corresponds to an observation, x_i , and the integer i if it corresponds to the latent unit z_j . The input mask element $M_{i,j}^{(w)}$ represent a connection from the i th input unit to the j th hidden unit. Thus we set $M_{i,j}^{(w)} = 1$ only when the integer assigned to the i th input is less than the integer assigned to the j th hidden unit, and 0 otherwise. In this way, if the j th hidden unit is assigned k , it will depend on $\{z_1, \dots, z_{k-1}, \mathbf{x}\}$. The output mask $M^{(v)}$ is constructed similarly by assigning the integer i the units corresponding to the parameters of q_i .

This method can be easily extended to feedforward networks with more than one hidden layer. For instance, if there is a second hidden layer \mathbf{h}' with mask $M^{(w')}$, we assign each hidden unit h'_i an integer uniformly from $\{1, \dots, m-1\}$ (or in fact, we can start from the lowest integer assigned to an h_i), and set $M_{i,j}^{(w')} = 1$ only when the integer assigned to h_i is less than or equal to the integer assigned to h'_j . In this way, if h'_j is assigned integer k , it depends on $\{z_1, \dots, z_{k-1}, \mathbf{x}\}$ through hidden units $\{h_i\}$ assigned k , it depends on $\{z_1, \dots, z_{k-2}\}$ through hidden units $\{h_i\}$ assigned $k-1$, and so on. This is a form of weight sharing.

We use two hidden layer MADEs in our experiments, including, in addition, masked skip-weights from the inputs to the outputs, as is recommended in Germain et al. (2015).

E.2 Tree MADE

In trying to model the regular but less-than-fully-connected dependency structure of minimally faithful inverses to binary trees, we had the following novel insight. Rather than thinking of the integers assigned to the input, hidden, and output units as simply numbers, we recognize that they actually identify subsets of the model variables. That is, k corresponds to $\{z_0, \dots, z_{k-1}, \mathbf{x}\}$. The mask weight is set to 1 only when the first subset is contained in the second. A difference choice of subsets will allow us to model another dependency structure, with the subset inclusion relationship defining weight sharing across the factors.

Running our algorithm on the binary tree Gaussian network of §3.2, reveals that one minimally faithful inverse for a model of depth d comprises factors,

$$q_i(x_i | x_{i+1}, \dots, x_{2(i+1)}), \quad i = 0, 1, \dots, 2^d - 2.$$

We break up the subsets $\{x_{i+1}, \dots, x_{2(i+1)}\}$ into,

$$\begin{aligned}&\{x_{i+1}\}, \\ &\{x_{i+2}, \dots, x_{2(i+1)}\}, \\ &\{x_{i+3}, \dots, x_{2(i+1)}\}, \\ &\vdots \\ &\{x_{2i+1}, \dots, x_{2(i+1)}\}\end{aligned}$$

for each i , and assign each a unique integer. The hidden units are uniformly assigned one of these subsets. The input unit for x_i is assigned the subset $\{x_i\}$ and the output units for the parameters of q_i are assigned the subset $\{x_{i+1} \dots, x_{2(i+1)}\}$. The mask from one hidden, input, or output unit to another is set to 1 only when the subset corresponding to the first unit is contained in the subset corresponding to the second unit.

By construction, this feedforward network will give the parameters for the $\{q_i\}$ such that $q(\mathbf{z} | \mathbf{x})$ is a minimal I-map for the posterior. This idea can clearly be generalized to arbitrary dependency

structures, which we leave for future work. We can algorithmically determine the form of the inverse factors in a minimally faithful inverse offline, extract all subsets of their scopes, and perform the same procedure as above.

F Theory

Here, we examine the complexity of the inversion problem and prove the correctness of NaMI’s graph inversion.

F.1 Inversion complexity

To understand the theoretical gains we obtain, it is useful to compare it with a simpler, but suboptimal, alternate that uses the d-separation properties of a BN structure to form a minimally faithful inverse. By the general product rule, any distribution over $\mathbf{y} = \{y_1, \dots, y_n\}$ can be factored as $p(\mathbf{y}) = \prod_{i=1}^n p(y_i \mid y_1, \dots, y_{i-1})$, for any ordering of \mathbf{y} . The conditioning sets, $\{y_1, \dots, y_{i-1}\}$, can be restricted according to the conditional independence assertions made by p . To produce a minimal I-map, they can be restricted as $p(\mathbf{y}) = \prod_{i=1}^n p(y_i \mid \tilde{\mathbf{y}}_i \subseteq \{y_1, \dots, y_{i-1}\})$ where $\tilde{\mathbf{y}}_i$ is a minimal subset such that $y_i \perp (\{y_1, \dots, y_{i-1}\} \setminus \tilde{\mathbf{y}}_i) \mid \tilde{\mathbf{y}}_i$.

Consequently, one could instead produce a minimally faithful inverse for $p(\mathbf{z} \mid \mathbf{x})p(\mathbf{x})$ as follows. Set $\mathbf{y} = (\mathbf{z}, \mathbf{x})$ to have an arbitrary topological ordering on \mathbf{z} and \mathbf{x} , separately. Initialize $\tilde{\mathbf{y}}_i = \{y_1, \dots, y_{i-1}\}$. Scan through $y_j \in \tilde{\mathbf{y}}_i$, removing each one if $y_i \perp y_j \mid \tilde{\mathbf{y}}_i \setminus \{y_j\}$, repeating until none can be removed and $\tilde{\mathbf{y}}_i$ is a minimal subset.

In the worst case for this naive approach, we must scan through $O(n^2)$ variables n times, and the cost of determining whether to remove a variable from $\tilde{\mathbf{y}}_i$ is $O(n)$ (Koller & Friedman, 2009, Algorithm 3.1). Thus, this naive method has running time $O(n^4)$. NaMI’s graph reversal, in contrast has a running time of order $O(nc)$ where n is the number of variables in the graph and $c \ll n$ is the size of the largest clique in the induced graph.

F.2 Proof of correctness

Theorem 2. *The Natural Minimal I-Map Generator of Algorithm 1 produces inverse factorizations that are natural and minimally faithful.*

Proof. As in the main paper, let τ denote the reverse of the order in which variables were selected for elimination such that τ is a permutation of $1, \dots, n$ and $\tau(n)$ is the first variable eliminated.

We first show that inverse structure \mathcal{H} produced by Algorithm 1 is guaranteed to be a valid inverse factorization, that is, it factors as

$$q_\psi(\mathbf{z} \mid \mathbf{x}) = \prod_{i=1}^n q_i(z_{\tau(i)} \mid \text{Pa}_{\mathcal{H}}(z_{\tau(i)})) = \prod_{i=1}^n q_i(z_{\tau(i)} \mid \text{Pa}_{\mathcal{H}}(z_{\tau(i)}), \mathbf{x}) \quad (1)$$

where \mathbf{z} and \mathbf{x} are the observed and latent variables, and $\text{Pa}_{\mathcal{H}}(z_{\tau(i)}) \subseteq \{\mathbf{x}, z_{\tau(1)}, \dots, z_{\tau(i-1)}\}$ indicates the parents of $z_{\tau(i)}$ in \mathcal{H} . There are two critical features this factorization encapsulates that we need to demonstrate to show \mathcal{H} provides a valid inverse factorization: \mathbf{x} only appears in the conditioning variables (i.e. there are no density terms over observations) and all terms can, if desired, be conditioned on the full set of observations.

The former of these straightforwardly always holds, since we only add edges *into* latent variables when the inverse, \mathcal{H} , is constructed (Line 11 in Algorithm 1). Therefore, the algorithm can never add in edges *to* an observed node.

The latter is more subtle, as NaMI may produce factors which are not explicitly conditioned on all the observations. However, because, as we demonstrate later, the inversion is faithful, the corresponding $z_{\tau(i)}$ must be conditionally independent of the all observations which are not parent nodes, given the state of the parent nodes. In other words, if the inversion is faithful, this ensures that each $q_i(z_{\tau(i)} \mid \text{Pa}_{\mathcal{H}}(z_{\tau(i)})) = q_i(z_{\tau(i)} \mid \text{Pa}_{\mathcal{H}}(z_{\tau(i)}), \mathbf{x})$, and thus that we have a valid inverse factorization.

Next, we prove that Algorithm 1 produces natural inverses. A general observation is that if z_i is eliminated after z_j , there cannot be an edge from z_j to z_i in \mathcal{H} . When the algorithm is run

in topological mode, variable elimination is simulated in a topological ordering, and so all of a variable’s descendants are eliminated after it is. Therefore there cannot be an edge from a variable to its descendant, and hence the factorization is natural. An equivalent argument applies when the algorithm is run in the reverse topological mode.

Finally, we prove that the inverse factorization is minimally faithful. At a high-level, our proof consists of showing an equivalence to a process where we start with a fully connected graph over the variables and sequentially prune edges in the graph according to the independencies revealed by the clique tree generated from simulating variable elimination, terminating when no more edges can be pruned. By showing that each individual pruning never induces an unfaithful independence, we are able to demonstrate that the graphs at each iteration of this process—including the final inverse graph—is faithful, while minimality follows from the fact that the process terminates when it is not possible to prune any given edge.

More precisely, by the general product rule, $p(\mathbf{z}|\mathbf{x}) = \prod_{i=1}^n p(z_{\tau(i)}|z_{\tau(<i)}, \mathbf{x})$, where $z_{\tau(<i)} = \{z_{\tau(1)}, \dots, z_{\tau(i-1)}\}$, for any possible τ , and any graph with this factorization is an I-map for the posterior. Each term can be simplified according the conditional independencies encoded by the posterior and the corresponding graph will still be an I-map for the posterior. For instance, if $z_{\tau(i)}$ is independent of $\{z_{\tau(1)}, \dots, z_{\tau(i-2)}\}$ given $\{z_{\tau(i-1)}, \mathbf{x}\}$, then $p(z_{\tau(i)}|z_{\tau(<i)}, \mathbf{x}) = p(z_{\tau(i)}|z_{\tau(i-1)}, \mathbf{x})$. By definition, the variable elimination is run in the opposite order to τ . This produces a unique corresponding clique tree (see Appendix A.5). Furthermore, because we introduce a new factor at each iteration, the number of cliques in this clique tree matches the number of latent variables in the original BN, with each clique being associated with the corresponding variable that was eliminated at that iteration (though the clique itself may contain multiple variables). We can thus define $C_{\tau(i)}$ as the unique clique corresponding to the elimination of $z_{\tau(i)}$. Further, we can define $S_{\tau(i)}$ as the sepset between $C_{\tau(i)}$ and $C_{\tau(i+1)}$, i.e. the set of variables shared between these two cliques. By the correspondence between clique trees and induced graphs, $S_{\tau(i)}$ is exactly the unmarked neighbours of $z_{\tau(i)}$ in the partially constructed induced graph at step $n + 1 - i$. Therefore, setting the parents of $z_{\tau(i)}$ to be its unmarked neighbours in Line 11 of Algorithm 1 constructs \mathcal{H} with the factorization

$$q_{\psi}(\mathbf{z} | \mathbf{x}) = \prod_{i=1}^n q_i(z_{\tau(i)} | S_{\tau(i)}), \quad (2)$$

which is of the form of (1) with $\text{Pa}_{\mathcal{H}}(z_{\tau(i)}) = S_{\tau(i)}$.

By construction, all $z_{\tau(>i)} = \{z_{\tau(i+1)}, \dots, z_{\tau(n)}\}$ are upstream in the clique tree from $z_{\tau(i)}$ (and thus downstream in the factorization), meaning they will never be included by $S_{\tau(i)}$. Furthermore, the sepset property of clique trees (Koller & Friedman, 2009, Theorem 10.2) guarantees that $z_{\tau(i)}$ is independent from $z_{\tau(<i)} \setminus S_{\tau(i)}$ given $S_{\tau(i)}$. Therefore, we have that $p(z_{\tau(i)} | S_{\tau(i)}) = p(z_{\tau(i)} | z_{\tau(<i)}, \mathbf{x})$ for each variable and so

$$p(\mathbf{z} | \mathbf{x}) = \prod_{i=1}^n p(z_{\tau(i)} | z_{\tau(<i)}, \mathbf{x}) = \prod_{i=1}^n p(z_{\tau(i)} | S_{\tau(i)}). \quad (3)$$

This is the same as the factorization produced by NaMI, as given in (2), and so we conclude that \mathcal{H} is an I-Map of \mathcal{G} and thus a faithful inverse.

The minimality now follows from the fact that the sepset $S_{\tau(i)}$ is also the minimal separating set (see, e.g., the proof of (Koller & Friedman, 2009, Theorem 4.12)). In other words, for each i , there is no $T_i \subsetneq S_{\tau(i)}$ such that $p(z_{\tau(i)} | T_i) = p(z_{\tau(i)} | S_{\tau(i)})$. Suppose we were to remove an edge, $z_{\tau(i)} \leftarrow y_j$, from \mathcal{H} , where $y_j \in \{\mathbf{x}, z_{\tau(<i)}\}$ (remembering that by construction we have no edges from $z_{\tau(>i)}$ to $z_{\tau(i)}$). This edge would have been constructed due to sepset $S_{\tau(i)}$. If removing the edge did not make \mathcal{H} unfaithful to \mathcal{G} , then this would imply that $p(z_{\tau(i)} | S_{\tau(i)} \setminus \{y_j\}) = p(z_{\tau(i)} | S_{\tau(i)})$ as none of the other factors will change. But we have already shown this is not possible. Hence, by contradiction, \mathcal{H} is minimally faithful. \square

References

- Germain, Mathieu, Gregor, Karol, Murray, Iain, and Larochelle, Hugo. MADE: masked autoencoder for distribution estimation. *Proceedings of the International Conference on Machine Learning*, 2015.
- Kingma, Diederik and Ba, Jimmy. Adam: A method for stochastic optimization. *arXiv preprint arXiv:1412.6980*, 2014.
- Kingma, Diederik P, Mohamed, Shakir, Jimenez Rezende, Danilo, and Welling, Max. Semi-supervised learning with deep generative models. In *Advances in Neural Information Processing Systems*, pp. 3581–3589, 2014.
- Koller, Daphne and Friedman, Nir. *Probabilistic Graphical Models*. MIT Press, 2009. ISBN 9780262013192.
- Maddison, Chris J, Mnih, Andriy, and Teh, Yee Whye. The Concrete distribution: A continuous relaxation of discrete random variables. In *International Conference on Learning Representations*, 2017.
- Paige, Brooks and Wood, Frank. Inference networks for Sequential Monte Carlo in graphical models. In *Proceedings of the International Conference on Machine Learning*, 2016.
- Stuhlmüller, Andreas, Taylor, Jacob, and Goodman, Noah. Learning stochastic inverses. In *Advances in Neural Information Processing Systems*, 2013.